Computational and Molecular Modeling Evaluation of the Structural Basis for Tubulin Polymerization Inhibition by Colchicine Site Agents

Ernst ter Haar,[a,†] Herbert S. Rosenkranz,[a,b] Ernest Hamel[c] and Billy W. Day[a,b,d,*]

[a]*Department of Environmental and Occupational Health, University of Pittsburgh Cancer Institute, University of Pittsburgh, 260 Kappa Drive, Pittsburgh, PA 15238, U.S.A.*

[b]*University of Pittsburgh Cancer Institute, University of Pittsburgh, 260 Kappa Drive, Pittsburgh, PA 15238, U.S.A.*

[c]*Laboratory of Molecular Pharmacology, Developmental Therapeutics Program, Division of Cancer Treatment, National Cancer Institute, National Institutes of Health, Bethesda, MD 20892, U.S.A*

[d]*Department of Pharmaceutical Sciences, University of Pittsburgh, 260 Kappa Drive, Pittsburgh, PA 15238, U.S.A.*

Abstract—The computer-automated structure evaluation programs MultiCASE and CASE were used to perform a quantitative structure–activity relationship study on tubulin polymerization inhibitors. A learning set of 536 chemicals (202 active, 27 marginal, and 307 inactive), built using IC_{50} values for inhibition of tubulin polymerization or mitosis from this and previous studies, was used for artificial intelligence self-teaching. The algorithms successfully predicted the activity of agents in the learning set with >90% accuracy. Seventeen MultiCASE and twelve CASE (mostly included in the MultiCASE set) biophores (substructures significantly correlated with activity) were identified with a probability >0.95. Here we present the biophores of podophyllotoxins, colchicinoids, and certain combretastatins, each examined for structure–activity relationships. For the podophyllotoxins and colchicinoids in the learning set, the correlations between observed and predicted potencies were >0.85. The algorithms recognized the importance of several known site, electronic, and steric effects in the two classes. A predictive QSAR ($R^2 = 0.98$) was developed for combretastatin A-2 and dihydrocombretastatin analogues. The MultiCASE/CASE analyzes were used in combination with molecular models to study relative orientations of colchicine, podophyllotoxin, combretastatin A-4, and steganacin at the colchicine site. This resulted in a new hypothesis, consistent with extensive published experimental data, in which the C-ring and part of the B-ring of colchicine overlap with the A- and B-rings of podophyllotoxin. Consequently, the trimethoxyphenyl rings of colchicine and podophyllotoxin occupied different regions of space, each pointing out from a hydrophobic 'core' occupied by the overlapping biophores. The molecular model of the highly potent combretastatin A-4 could fit into the model binding site in at least three different ways. The developed QSARs were used to identify the potent microtubule stabilizer discodermolide. Its identification, in concert with recently reported findings, suggest potential overlap in the colchicine and paclitaxel binding sites on tubulin. Copyright © 1996 Elsevier Science Ltd

Introduction

Drugs that inhibit tubulin polymerization/depolymerization are currently under study or commonly used as chemotherapeutic agents for a variety of cancers, as well as for probing microtubule dynamics in cellular and biochemical processes. Well-known examples are vinblastine, vincristine, and paclitaxel. The class of molecules that alter the ability of tubulin to polymerize/depolymerize do not constitute a data base of congeneric structures, nor are their interactions with tubulin the same. For example, paclitaxel, *Vinca* alkaloids, colchicinoids, and dolastatin 10 appear to bind at different sites on the tubulin α-β heterodimer.[1]

The colchicine binding site, the most extensively studied in terms of structure–activity relationships (SARs), can be occupied by structurally diverse

compounds. It is known that podophyllotoxin and combretastatin A-4 analogues also bind at this site.[2,3] Various studies have analyzed the binding mechanism of these compounds and conclude that the binding of colchicine and podophyllotoxin to tubulin is dissimilar.[4,5] The interaction of colchicine with tubulin is 'irreversible' and temperature-sensitive. Podophyllotoxin binds faster than colchicine and the binding is reversible and less temperature-sensitive. Following binding of podophyllotoxin, the GTP hydrolyzing capacity of tubulin is inhibited, but colchicine stimulates an assembly-independent GTPase activity directed at the exchangeable site-bound GTP.[6,7]

Podophyllotoxin analogues can roughly be divided into two groups. The first has tubulin polymerization inhibitory activity (e.g. podophyllotoxin) and the second has DNA topoisomerase II inhibitory activity (e.g. etoposide). The most important structural difference between the two groups is the presence of a (bulky) glucoside moiety in the axial position of ring C for topoisomerase II inhibitors and a (small) equatorial

†Present address: Department of Cell Biology and The Center for Blood Research, Harvard Medical School, Boston, MA 02115, U.S.A.

substituent for tubulin polymerization inhibition (TPI) activity. Modification of the equatorial 4-hydroxyl group of podophyllotoxin has minor consequences for TPI activity. Changes at the lactone D-ring, however, have a large effect on potency.[8,9] The trimethoxyphenyl ring of podophyllotoxin (the E-ring) is pseudoaxial, pendant to the C-ring. Little has been reported in the SAR of alterations in the podophyllotoxin E-ring, and the results from such studies are not in agreement.[8-11]

Many analogues of colchicine have been synthesized and analyzed for TPI activity. Most of the structural changes reported are at the A-ring, C_7-, and C_{10}-sites.[12-15] SAR studies suggest that the interaction of tubulin with the C_7-site are mostly electronic in nature[12,13] and interaction with the C_{10}-site is sterically controlled.[15]

Combretastatins, originally isolated from the South African tree *Combretum caffrum*, are structurally the most simple and among the most potent natural products that inhibit tubulin polymerization. Although many analogues have been described, two have received the most attention: combretastatin A-2 and combretastatin A-4.[2] The binding of the latter to tubulin is temperature-independent and stimulates GTPase activity, while the former has little effect on GTPase activity.[3] SAR studies carried out on combretastatins show that the 4'-methoxy substituent on the B-ring is important for TPI activity.[16,17] The only way found to increase their TPI activity is an additional hydroxyl group at the 2' position. This is also true for the dihydro analogues of combretastatin A-4.

The increase in available databases as a result of standardized assays for toxicity, mutagenicity, carcinogenicity, and pharmaceutical effects, and the rapid development in artificial intelligence has made QSAR a valuable tool in analyzing biological responses. Here we describe the use of two related computational artificial intelligence QSAR programs, MultiCASE and CASE,[18,19] to study the structural basis for tubulin polymerization inhibition. Many compounds have been tested for TPI activity in standard assays; this makes them suitable for analysis with MultiCASE and CASE. Since there are multiple sites for compounds to bind to tubulin and interfere with polymerization/depolymerization, not all compounds will have the same binding mechanism. It is thus likely that the classes of compounds binding at different sites on tubulin will have different structure–activity relationships. Compounds that bind at the same or overlapping sites should, however, have some common structural features responsible for activity. MultiCASE and CASE can identify those subsets of compounds by grouping them under different 'biophores', substructural features statistically correlated with activity. The results of the MultiCASE and CASE analyses were used to obtain mechanistic insight into the interaction between the compounds and the colchicine binding site of tubulin and to search for antitubulin compounds not previously described to have this activity.

Results

CASE/MultiCASE analysis

The CASE program[18] generates, from each molecule in the learning set, substructural fragments by subdividing the molecule into all possible fragments of 2–10 contiguous nonhydrogen atoms. Each fragment from an inactive molecule is labeled inactive, and each fragment from an active molecule is labeled active, then weighted with its assigned activity after replacement of the hydrogens. The fragments are processed statistically by using binomial distribution criteria and Bayesian probability values, and only the most statistically significant fragments are retained. Thus, each fragment not related to activity will be found randomly in active and inactive molecules. Any deviation from random distribution, at a 95% confidence level, indicates that the fragment is relevant to the observed activity. The result is a collection of substructures presumed to be responsible for the observed activity of the molecules in the learning set. These substructures were used to calculate the probability of TPI activity.

MultiCASE[19] identifies the substructural fragment responsible for the activity of the largest group of chemicals in the learning set (biophore) and then invokes structural and physicochemical modulators to explain differences in actual potency. Such modulators include substituents, octanol/water partition coefficients (log P), lowest unoccupied and highest occupied molecular orbitals (LUMO, HOMO). Log P, for example, was invoked in this study to account for transfer of a ligand from the aqueous phase to the lower dielectric constant 'protein' phase, since the data for compounds in the learning set came largely from tests with isolated tubulin. After identifying the biophore, MultiCASE removes those chemicals containing it from further consideration and repeats this process until the activity of most of the chemicals in the learning set can be explained by multivariate linear regression analysis of each biophore/modulator subset. Since the biophores generated by CASE/MultiCASE are two-dimensional in nature, the algorithms do not discriminate between stereoisomers (hence, figures depicting biophores are intentionally shown without known stereochemistry of the agents), but do recognize geometric isomers.

The MultiCASE and CASE programs can also predict the potency of chemicals after a statistically significant analysis of each biophore and biophobe has been achieved. They evaluate each biophore by linear regression analysis and the most relevant biophores are chosen through a forward selection process. This results in the election of the minimum number of descriptors necessary to calculate the potency of the chemicals.

A learning set of 536 chemicals tested for tubulin polymerization inhibition was assembled. Their potencies and chemical structures were obtained from several literature sources or were generated in this study[2,8,10,14–17,20–34] and were uniformly adjusted to in

vitro TPI IC_{50} (μM) values relative to a historic IC_{50} value for colchicine (2.4 μM). For certain chalcones in the learning set,[20] an equivalent value based on anti-mitotic effects compared with that of 0.05 $\mu g/mL$ colchicine was calculated. The chemicals were subjected to MultiCASE and CASE analyses to generate biophores (activating fragments), biophobes (inactivating fragments), and physicochemical modulators associated with probability of activity. Their activities were classified as follows: 202 as active ($IC_{50} < \sim 11$ μM), 307 as inactive ($IC_{50} > 13.5$ μM), and 27 as marginally active. These IC_{50} cut-off values were iteratively chosen to distribute the compounds into the three groups so that the analyses would be biased toward the recognition of only those substructural fragments most statistically significant for activity. The chemical classes included 59 colchicinoids and allocolchicinoids, 21 podophyllotoxins, 72 chalcones, 47 benzyl benzodioxoles, 17 steroids, 89 stilbenes and combretastatins, 73 phenylquinolones, 36 styrylquinazolinones, 8 phenanthrenes, 16 benzyl anilines, and 98 miscellaneous agents. Several compounds could be considered members of more than one class.

The CASE analysis resulted in the selection of 12 fragments (biophores) that had a statistically significant association with TPI activity (Table 1). The Multi-CASE analysis resulted in the selection of 17 biophores (Table 2), five of which were also selected by CASE. For example, MultiCASE biophore 1 was also selected by CASE (biophore 4) and was found in 41 colchicinoids and in aminopodophyllotoxin. Each of these fragments was characterized by its distribution among active, inactive and marginally active molecules, and the confidence level (P value) associated with it. The presence or absence of these fragments was used to predict the likelihood of the given compound being a tubulin polymerization inhibitor. The combined analysis of the chemicals in the learning set by the two algorithms resulted in a sensitivity of 0.92, a specificity

of 0.96 and a correlation between the predicted and observed potencies of 0.95 (values greater than obtained with either algorithm singly). Localization of biophores in selected active molecules are shown in Figures 1 and 2.

The MultiCASE and CASE programs generated considerable information in the form of biophores that may explain the TPI effect of the chemicals. Although the two algorithms are different, the biophores generated by both were very similar. The biophores with the highest probability were found in the chemical families with the most potent inhibitors, colchicinoids, podophyllotoxins, and combretastatins.

MultiCASE and CASE can be used to predict the probability of activity and potency of structures not present in the learning set, based on the presence of biophores identified by the algorithms. If none of these biophores are present in a queried structure, the MultiCASE/CASE programs give only the probability of activity. We did a QSAR study of colchicinoids, podophyllotoxins and combretastatins that were not in the learning set and compared the results with published data on colchicine binding inhibition (CBI) or TPI. In these studies we found that the average of the potencies predicted by MultiCASE and CASE was more useful than that predicted by either algorithm alone. The statistical portion of the CASE/MultiCASE analysis was reexamined with the statistical packages SAS and BMDP4R to ensure that the resulting QSAR equations and our applications of them were statistically valid and not 'overfit'.

QSAR of colchicinoids

Two MultiCASE biophores and five CASE biophores present in the colchicinoids (one biophore in both sets) were selected by the forward selection method to calculate their potencies (Fig. 3). These biophores

Table 1. Major CASE biophores associated with the inhibition of tubulin polymerization[a]

Fragment ------1-------2-------3-------4-------5-------6-------7-------8-------9-------10---------SUB	No. of Fragm.	Inact.	Marg.	Active	Prob.
1. CH″—CH =C. —C. =	58	9	1	48	<0.001 + + +
2. CH₂—CH₂—CH —C. =	44	3	1	40	<0.001 + + +
3. CO —O —CH₂—CH —CH₂—	5	0	0	5	0.031 + + +
4. CH₂—CH₂—CH —C. =CH — <3-NH>	41	2	1	38	<0.001 + + +
5. N —C =CH —CH =C —CH =	30	4	2	24	<0.001 + + +
6. OH —C =C —CH =CH —C″ —CH₂— <3-O>	11	2	0	9	0.019 + + +
7. CH₂—O —C. =CH —C =C —CH = <5-O>	13	1	0	12	0.001 + + +
8. O —C. =CH —C =C —CH =C. —O — <4-O>	12	1	0	11	0.002 + + +
9. NH —CH —C. =CH —CO —C =CH —CH = <6-S>	19	0	0	19	<0.001 + + +
10. CH₃—O —C =C —CH =C —CH =CH —C =	24	5	1	18	0.003 + + +
11. CH =CH —CH =CH —C =C —NH —C. =CH — <5-CH=>	10	2	0	8	0.033 + + +
12. CH =CH —CH =CH —CH =C —C″ —NH —C. =CH —	10	2	0	8	0.033 + + +

[a]C. Indicates a carbon atom common to two rings. C″ Indicates a substituted carbon. SUB indicates a substituent on the biophore, e.g. <3-NH> is an NH on position 3 from the left. The table lists the number of times the fragment was encountered in the learning set and its distribution among active, inactive and marginally active molecules. This distribution was used to predict the likelihood that the presence of that fragment contributes to the inhibition of tubulin polymerization. Also listed in the table are the probability values associated with the significance of these distributions: + + +, $p < 0.01$ (F-test). Localization of the fragments in selected molecules are shown in Figure 1.

Table 2. Major MultiCASE biophores associated with the inhibition of tubulin polymerization[a]

Fragment -------1-------2-------3-------4-------5-------6-------7-------8-------9-------10-----------------SUB	No. of Fragm.	Inact.	Marg.	Active	Average IC_{50}
1. CH_2—CH_2—CH —C. =CH — <3-NH>	41	2	1	38	3.0 +++
2. CH_3—N —C =CH —CH =C —CH=	24	2	2	20	5.6 +++
3. CH_2—O —C. =CH —C =C —CH = <5-O>	13	1	0	12	5.1 +++
4. CH_3—O —C =C —CH =C —CH =CH —C = <3-C=>	22	4	1	17	5.9 +++
5. OH —C =C —CH =CH —C" —CH_2— <3-O>	11	2	0	9	5.4 +++
6. CO —O —CH_2—CH —CH_2—	5	0	0	5	2.1 +++
7. CH =CH —CH =CH —C =C —NH —C. =CH — <5-CH=>	10	2	0	8	6.6 +++
8. CH_3—CH_2—N —C =CH —CH =C —	6	1	0	5	5.1 ++
9. OH —CH —C. =CH —C."—O —	5	1	0	4	5.9 +
10. O —CH_2—O —C. =CH —C."—CH_2—CH —CH_2—	7	1	0	6	5.0 +++
11. O —C =CH —C."—CO —NH —C" —CH =CH — <7-N=>	4	1	0	3	5.9
12. O —CH_2—O —C. =CH —C =CH —	6	1	0	5	4.2 ++
13. S —C =CH —CH =C. —C. =C —C =C —O — <7-O>	29	6	0	23	4.5 +++
14. NH —C =CH —CH =C —CH =CH — <5-O>	4	0	2	2	9.3
15. CH =CH —CH =CH —C =C —NH —C. =CH —C. =	4	1	0	3	5.3
16. O —C =C —CH =C —CO —C = <3-O>	5	0	0	5	5.0 +++
17. C =CH —CH"—CO —C =C —C =C — <6-O>	4	0	0	4	6.5 ++

[a]C. Indicates a carbon atom common to two rings. C" Indicates a substituted carbon. SUB indicates a substituent on the biophore, e.g. <3-NH> is an NH on position 3 from the left. The table lists the number of times the fragment was encountered in the learning set and its distribution among active, inactive and marginally active molecules. This distribution was used to predict the likelihood that the presence of that fragment contributes to TPI activity: $+, p < 0.125$; $+ +, p < 0.05$; $+ + +, p < 0.01$ (F-test). Also listed in the table are the average IC_{50} values of the molecules containing the given fragment. Localization of fragments in selected molecules are shown in Figure 2.
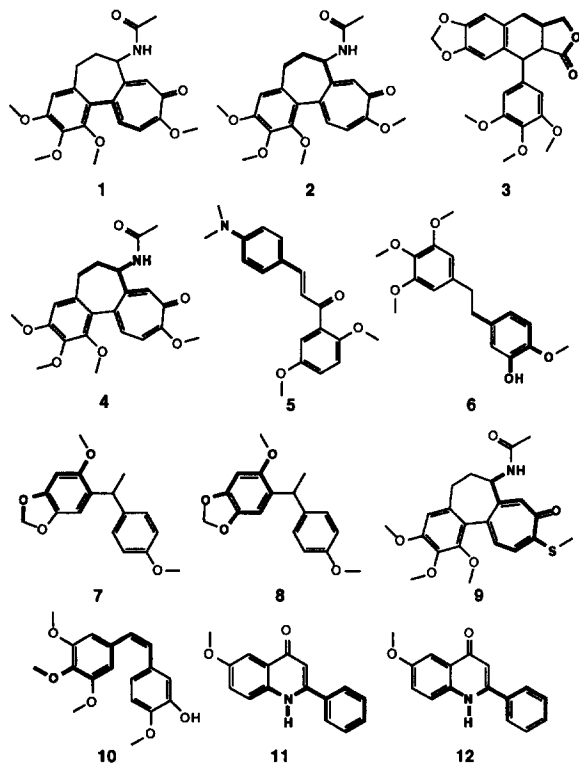

Figure 1. Examples of the 12 biophores (bold) identified by CASE: **1, 2, 4**: colchicine; **3**: deoxypodophyllotoxin; **5**: E-1-(2,5-dimethoxy-phenyl)-3-[4'-(dimethylamino)-phenyl]-2-methyl-2-propen-1-one; **6**: dihydrocombretastatin A-4; **7, 8**: NSC 350102; **9**: thiocolchicine; **10**: combretastatin A-4; **11, 12**: 6-methoxy-2-phenyl-4-quinolone. Note: known stereochemistry of the chemicals is intentionally not shown in Figures 1–5 and 7 (see second paragraph of Results).

accounted for 85% of the activity of the compounds, as shown by comparing predicted versus observed potencies [Fig. 4(A)]. One MultiCASE biophore was a substructure of the B- and C-rings and included the nitrogen bound to the C_7-carbon (Fig. 3). Three of the four CASE biophores that were substructures of the B- and C-rings also included the nitrogen of the C_7-substituent. In all these biophores, however, the remainder of the C_7-substituent was not part of the activating fragment identified, indicating that the electron pair of nitrogen influences the interaction between tubulin and colchicine, while the size of the C_7-substituent does not. Many colchicinoids with modified C_7-substituents have been tested for TPI[15] and CBI.[12,13] Earlier SAR studies of colchicine analogues have shown that different substituents at the C_7-position only have a minor influence on TPI activity.[12,13] Analogues with bulky substituents are still very potent. For example, speciocine inhibits the binding of colchicine to tubulin by 62%. Analogues with an electronegative substituent, such as N-deacetyl-N-(trifluoroacetyl)colchicine, inhibit the binding of colchicine by 100%. The strong activity of both compounds was correctly predicted by Multi-CASE and CASE. In fact, analogues without this substituent, where the C_6–C_7 linkage is —CH_2—CH_2—, =CH—CH_2—, or —CH=CH—, are also active polymerization inhibitors.[21,35] A study on the kinetics of colchicinoid–tubulin interaction using C_7-modified colchicine analogues has shown that the energy of activation of the conformational change in tubulin associated with colchicine binding is decreased when the C_7-substituent is removed, such as with deacetamidocolchicine, a potent TPI. Complete removal of the B-ring results also in a lower energy of activation due to free rotation of the A- and C-rings.[36]

A decrease in the size of the C_7-substituent has, however, little effect, leading to the conclusion that the size of the substituent plays only a minor role in the interaction with tubulin.[37] When the colchicine N-acetyl group is replaced by an N-ethoxycarbonyl or N-butoxy-carbonyl group, the TPI potency increases despite the increase in the size of the substituent. The activity of these N-alkoxycarbonyl compounds was correctly predicted by the algorithms (Fig. 5). Replacement of the nitrogen-bound hydrogen with a methyl increased predicted potency, while replacement of the N-acetyl with hydrogen (to give the primary amine) or with an N,N-dimethylamino group reduced predicted potency. These predictions were also in accord with experimental data.

Aminopodophyllotoxin shared the same MultiCASE biophore with 41 colchicinoids (biophore 1; Table 2, Fig. 2). This biophore had a high probability of being correlated with activity. In aminopodophyllotoxin, however, the secondary amine is replaced by a primary amine, and this change was associated with decreased predicted potency. The colchicine analogue containing the same biophore as podophyllotoxin, N-deacetylcol-chicine, has been tested for both CBI and TPI and found less potent than colchicine (CBI: 51% compared with 90% for colchicine; TPI: IC_{50} 3.3 μM versus 2.4 μM for colchicine).[12,38]

A second MultiCASE biophore (biophore 13; Table 2, Fig. 2) also was identified for explanation of the activity of colchicinoids. The structures containing it were thiocolchicines, and the biophore included both the thiomethyl group at the C_{10}-position and the C_1-methoxy group (Fig. 3). The CASE analysis identified a biophore in the same area of the colchicinoid structure (biophore 1; Table 1, Fig. 1). The C_1-substituent is considered important for the TPI activity of colchicine because it influences the conformation of the colchicinoid by steric interaction with the C_{12}-hydrogen.[39]

Several colchicinoids with modifications on the A-ring have been tested experimentally for TPI and CBI. Removal of the 3-methyl group causes a decrease in both the TPI and CBI potencies. 2-Demethylcolchicine and 1-demethylcolchicine have reduced potency in both assays. For example, 2-demethylcolchicine inhibits colchicine binding by 50% and 1-demethylcolchicine by 26% under the conditions cited.[13] The C_1-methoxy group was part of both CASE and MultiCASE biophores. Compounds lacking this substituent were predicted to be inactive. Those lacking only the C_1-methyl were not predicted to have different activities, contrary to what is found experimentally. Compounds lacking C_2- or C_3-methoxy substituents had high predicted potency. The compound with a methyl-enedioxy system in place of the two methoxy substituents had the same predicted activity. This compound is as potent as colchicine.[40] The predictions made by MultiCASE and CASE showed that the algorithms recognized the importance of the C_1-methoxy group. Also, the inclusion of the oxygen in the MultiCASE and CASE biophores indicated the importance of the free electron pairs at this position.

Figure 2. Examples of the 17 biophores (bold) identified by Multi-CASE: 1: colchicine; 2: E-1-(2,5-dimethoxyphenyl)-3-[4'-(dimethyl-amino)-phenyl]-2-methyl-2-propen-1-one; 3: NSC 321567; 4: combretastatin A-4; 5: dihydrocombretastatin A-4; 6: deoxypodo-phyllotoxin; 7: 6-methoxy-2-phenyl-4-quinolone; 8: E-1-(2,3,4-tri-methoxyphenyl)-3-[4'-(diethylamino)phenyl]-2-methyl-2-propen-1-one; 9: podophyllotoxin; 10: deoxypodophyllotoxin; 11: 6-methoxy-2-styrylquinazolin-4(3H)-one; 12: combretastatin A-2; 13: thio-colchicine; 14: N-(3',4',5'-trimethoxybenzyl)-4-methoxyaniline; 15: 6,7-dimethoxy-2-phenyl-4-quinolone; 16: E-1-(3,4,5-trimethoxy-phenyl)-3-[4'-(dimethylamino)-phenyl]-2-methyl-2-propen-1-one; 17: E-1-(2,3,4-trimethoxyphenyl)-3-[4'-(dimethylamino)-phenyl]-2-propen-1-one.

The structure–activity relationships found in an earlier study on alterations at the C_{10}-position[14] were compared with the MultiCASE and CASE analyses. In the cited study, 17 C_{10}-modified colchicinoids were analyzed. Most of them are potent TPIs despite the structural changes. Replacement of the C_{10}-methoxy with an electronegative substituent such as a halogen or with an alkyl group causes only small changes in experimental potency. The potency decreases, however, when the length of this substituent increases. The three compounds with the lowest potency have an isoprop-oxy, n-butyl, and a phenyl group at the C_{10}-position.
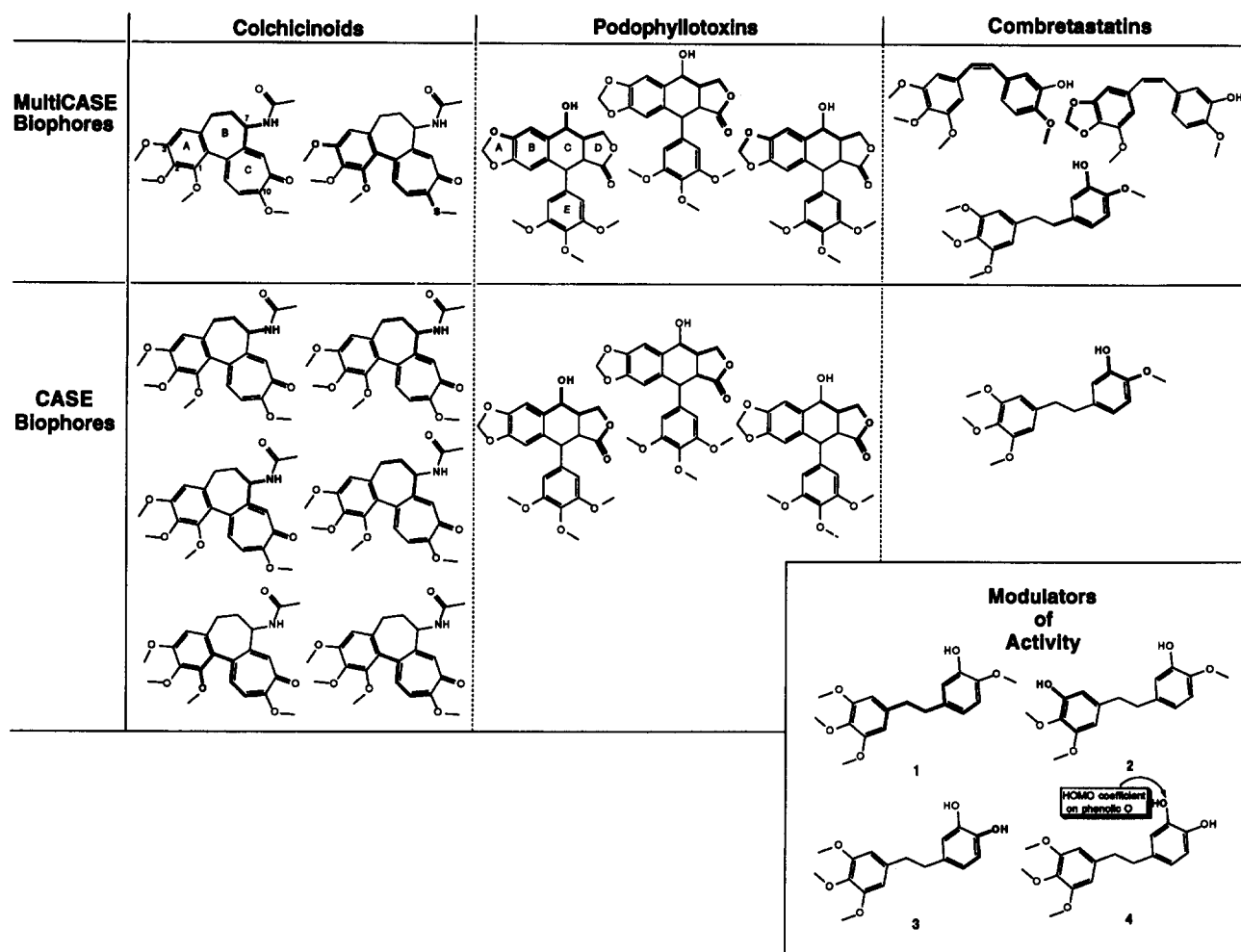
Figure 3. The MultiCASE and CASE biophores present in colchicinoids, podophyllotoxins, and combretastatins. The lower right of the figure depicts the four modulators of the MultiCASE biophore present in dihydrocombretastatins. Modulator 1 increased the predicted potency (i.e. decreased predicted IC_{50} by 1.05 µM) when present. The other three modulators decreased the predicted potency.
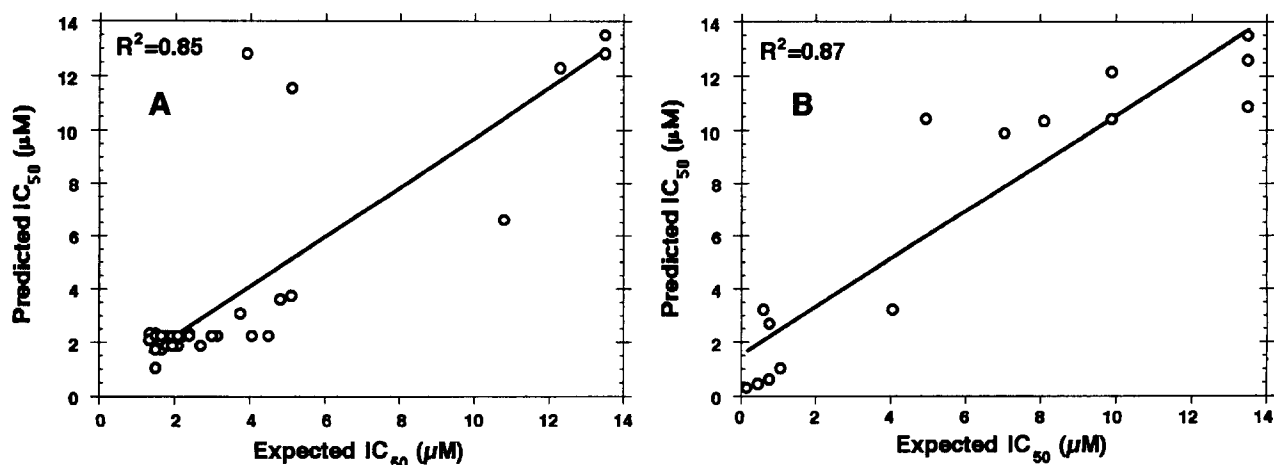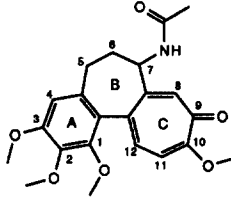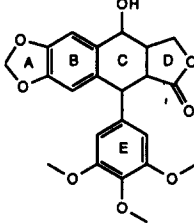

Figure 4. The computationally predicted potencies of the colchicinoids and podophyllotoxins in the learning set versus their experimental potencies obtained from literature sources. For the 59 colchicinoids (A), the correlation (R^2) was 0.85. For the 21 podophyllotoxins (B), R^2 was 0.87.

The positions of the 9-carbonyl and the 10-methoxy are important for the interaction with tubulin. Switching the carbonyl with the methoxy yields an inactive molecule, as has been found experimentally. Most of these experimental observations were reiterated when the learning set was queried by the algorithms. The major exception was that they did not predict the observed loss of activity with a C_{10}-propoxy group, although bulkier substituents were correctly predicted to reduce activity.

Colchicinoid	Predicted IC$_{50}$ (µM)	Experimental Activity
Colchicine	3.8	TPI 2.4 µM CBI 90%
N-(Trifluoroacetyl)-deacetylcolchicine	2.3	CBI 100%
Speciocine	8.7	CBI 62%
3-(Ethoxycarbonyl)-3-demethylthiocolchicine	2.3	TPI 1.4 µM
3-(Butoxycarbonyl)-3-demethylthiocolchicine	2.3	TPI 1.4 µM
N-Methylcolchifoline	1.4	CBI 98%
N-Deacetylcolchicine	8.7	CBI 51%
N-Methyldemecolcine	8.7	CBI 38%

Podophyllotoxin Analogue	Predicted IC$_{50}$ (µM)	Experimental Activity
Podophyllotoxin	3.2	TPI 0.6 µM
G4	9.3	TPI >50 M
Dehydropodophyllotoxin	>13.5	TPI >25 µM
Desoxypodophyllotoxin	0.5	TPI 0.5 µM
β-Peltatin	0.5	TPI 0.7 µM
Anhydropodophyllol	<0.15	TPI 1.0 µM
Picropodophyllic Acid	>13.5	CBI 0%
Podophyllic Acid 2-ethylhydrazide	>13.5	CBI 22%
Podophyllotoxin cyclic sulfide	12	TPI 10 µM
Podophyllotoxin cyclic sulfone	13.4	TPI >100 µM
4'-Demethylpodophyllotoxin	3.2	TPI 0.5 µM

Figure 5. QSAR studies on the C_7-substituent of colchicine and its analogues (*Left*) and on the C-, D-, and E-rings of podophyllotoxin and its analogues (*Right*). The experimental potencies are from literature sources and are the percent inhibition of colchicine binding inhibition (CBI) or the IC$_{50}$ value for tubulin polymerization inhibition (TPI).

QSAR of podophyllotoxins

MultiCASE selected three biophores for podophyllotoxin analogues (Fig. 3). One contained the lactone D-ring and the other two contained parts of the A-, B-, and C-rings, with the only difference being the presence of the 4-hydroxyl group. The CASE biophores for the podophyllotoxins were very similar to the MultiCASE biophores, but did not include the benzodioxole A-ring. None of the MultiCASE or CASE biophores included the E-ring of podophyllotoxin, undoubtedly due to the few E-ring-modified podophyllotoxin analogues in the learning set (only α-peltatin and 4'-demethylpodophyllotoxin, both with a hydroxy group at the E-ring para-position).

The activity of podophyllotoxins and benzyl-1,3-benzodioxole compounds have been compared because of their structural similarity, although the latter lack the C- and lactone D-rings.[23,41] The biophore identified by MultiCASE for the benzyl benzodioxole compounds included the methylenedioxy ring and the benzyl ring, much like two of the biophores identified in the podophyllotoxins. This means that MultiCASE and CASE considered the methylenedioxy- and the B-ring to be important for the interaction between podophyllotoxin analogues and tubulin. The selected biophores accounted for 86% of the potency of these compounds, as indicated by the predicted versus observed plot [Fig. 4(B)]. The activitites of the most potent podophyllotoxins (observed $IC_{50} < 3$ μM) were predicted most accurately.

Podophyllotoxins with modified C-rings that have been tested experimentally[8] for TPI activity were tested by MultiCASE and CASE (Fig. 5). The TPI potency (both experimental and predicted) was especially reduced when the C-ring was removed (G4) or was unsaturated (dehydropodophyllotoxin). When the C-ring's substituent was removed as in desoxypodophyllotoxin or replaced as in β-peltatin, however, the resulting analogue was still a potent inhibitor. This indicated that the three-dimensional conformation of the C-ring, and the resulting conformational influence on the D-ring, is important for interaction with tubulin. This concurs with the finding that stereoisomers like epipodophyllotoxin are much less potent.

The decreased potency of lactone D-ring analogues was also usually predicted by MultiCASE and CASE (Fig. 5). Only the minor reduction in activity that occurs with the removal of the lactone carbonyl was not recognized by the algorithms.

Few analogues with modifications on the E-ring have been tested in vitro for TPI (Fig. 5). Removal of the 4'-methyl to give the phenol results in a small increase in potency. An increase in potency is also seen when the C-ring hydroxyl is moved to ring B: α-peltatin is slightly more potent than β-peltatin. The influences of these structural modifications were correctly predicted by MultiCASE and CASE. The E-ring was not included in any biophore identified by the algorithms,

and structural changes in it had no large effects on the predicted potency of TPI.

QSAR of combretastatins

There were three biophores for the combretastatin analogues identified by MultiCASE and one identified by CASE (Fig. 3). The three MultiCASE biophores represented separate groups of the combretastatin class: combretastatin A-4 analogues, combretastatin A-2 analogues, and dihydrocombretastatin analogues. The CASE algorithm could not identify a fragment to explain the activity of the combretastatin A-4 analogues. The SAR of the combretastatin A-4 analogues was not well explained by the single MultiCASE biophore, resulting in an R^2 of the predicted versus the observed potency of only 0.17. Future QSAR studies on these simple but potent compounds will likely require the invocation of three-dimensional molecular and substituent electronic parameters to explain their activity.

Dihydrocombretastatins and combretastatin A2 derivatives were, however, well explained by CASE/MultiCASE analysis. The MultiCASE biophore for the dihydrocombretastatins overlapped with the CASE biophore and contained the B-ring and part of the saturated bridge. One modulator accompanying this biophore increased the predicted activity (Fig. 3). The modulator contained part of the B-ring and the C2-bridge. Its selection indicated the importance of the bridge length for the tubulin interaction and suggested, as has been shown,[2,22] that the ideal bridge length for these compounds to have TPI activity is two carbons. The combretastatin A-2 analogues have a methylenedioxy ring and, as with podophyllotoxins and benzyl benzodioxoles, this moiety was part of the biophore, which again stressed its importance for the interaction with tubulin. The R^2 of the predicted versus the observed potency of dihydrocombretastatins and combretastatin A-2 analogues combined was 0.98.

Discussion

Modeling of the colchicine binding site

Podophyllotoxin, steganacin, combretastatin A-2, and combretastatin A-4 all competitively inhibit the binding of colchicine to tubulin,[39] implying that these agents all bind to tubulin at the same site. The structural features these agents all share with colchicine is the trimethoxyphenyl moiety.

For colchicine and podophyllotoxin, it has been suggested that the binding sites for the two drugs do not completely overlap, with the trimethoxyphenyl rings of the agents binding in the same site on the tubulin heterodimer.[4,5] Others have found, however, that the SARs governing the trimethoxyphenyl regions in the colchicinoids and podophyllotoxins differ. Every sequential demethylation of the colchicine A-ring results in a decrease in TPI potency,[42] but there are

conflicting results about the effects of demethylation in the E-ring of podophyllotoxin derivatives. Some investigators have reported enhanced activity in 4'-demethylpodophyllotoxin relative to podophyllotoxin,[8,10] while others have found reduced activity in 4'-demethylpodophyllotoxin[10,43] and in 4'-demethyl-deoxypodophyllotoxin and 3',4'-demethyldeoxypodophyllotoxin.[44] In a series of compounds believed to be podophyllotoxin congeners, it was found that in benzyl-benzodioxole derivatives the 4'-monomethoxybenzene ring yielded maximum activity, while negligible activity occurred with a 3',4',5'-trimethoxybenzene ring;[23,41] in the methylenedioxybenzopyran series, in contrast, maximum activity was observed only with a 3',4',5'-trimethoxybenzene ring.[11]

To explore possible orientations of colchicine and podophyllotoxin at the colchicine binding site, we used the biophore results of the MultiCASE and CASE analysis and the hypothesis that these biophores are the portions of the structures of each chemical class that occupy the same region in space at the colchicine binding site. Molecular models of colchicine and podophyllotoxin were constructed with CHARMm and AM1, and the isoelectronic atoms in their shared MultiCASE biophores were maximally superimposed [Fig. 6(A)]. When this was done, the trimethoxyphenyl rings of the two drugs were situated in different regions of space, nearly orthogonal to each other. This suggested that these rings may bind to different regions of tubulin, and may explain a number of results obtained in the CASE/MultiCASE analyses: (1) only part of the A-ring of colchicine was represented in a biophore; (2) the E-ring of podophyllotoxin was not in a biophore; (3) there was only a single biophore shared by multiple colchicine analogues and a single podophyllotoxin analogue, although other podophyllotoxin analogues had an activating fragment in the corresponding region of their structures. The overlapping biophore was present in the C-ring of colchicine and the B-ring of the podophyllotoxin derivative.

Overlap of the combretastatin A-4 biophores with the biophores of colchicine and podophyllotoxin occurred in three energetically feasible ways. In the first, shown in Figure 6(B), the two aromatic rings of combretastatin A-4 overlapped with the trimethoxyphenyl moieties of colchicine and podophyllotoxin. In the second, the two rings of combretastatin A-4 overlapped with the methylenedioxy moiety and trimethoxyphenyl ring of podophyllotoxin. In the third, the aromatic rings of combretastatin A-4 overlapped with the methylenedioxy moiety of podophyllotoxin and the trimethoxyphenyl ring of colchicine. Since the two phenyl rings of the stilbene are interchangeable in these models, this represents up to six possible binding modes. If such multiple modes of interaction can occur on tubulin, this could underlie the potent activity of this structurally simple antimitotic compound. Moreover, it may explain the diverse effects of combretastatin derivatives on tubulin-dependent GTPase activity, with some derivatives stimulating hydrolysis (as

does colchicine), others inhibiting (as does podophyllotoxin), and others having little apparent effect.[45]

Steganacin can be considered a structural analogue of either podophyllotoxin or colchicine. Its biaryl configuration is the same as that in colchicine[46] and, in terms of its effects on tubulin-dependent GTP hydrolysis, it also acts as a colchicine analogue in that it stimulates the reaction.[23] When the energy minimized structures were superimposed in terms of common biophores [Fig. 6(C)], the trimethoxyphenyl ring of steganacin overlapped that of colchicine rather than that of podophyllotoxin. Moreover, the ester side chain of steganacin did not superimpose on the amide side chain of colchicine, consistent with the known SAR of these agents. While the amide substituent is not required for colchicinoid activity, the acetate side chain of steganacin is essential.[47]

In summary, the models of drug structural overlap in terms of CASE/MultiCASE biophores are speculative at present. Perhaps the most suggestive experimental evidence supporting the idea of two distinct modes of interaction of trimethoxyphenyl moieties with tubulin is the differing effects of 'colchicine site' drugs on tubulin-dependent GTP hydrolysis. Stimulation of the reaction occurs with colchicinoids, steganacin, some combretastatin derivatives (including combretastatin A-4), and methylenedioxy-benzopyran derivatives. Inhibition of GTP hydrolysis occurs with podophyllotoxin, benzylbenzodioxole derivatives, and some combretastatin derivatives. It should be noted that these differences in effects on GTP hydrolysis cannot be readily explained in terms of kinetics of drug binding or dissociation, inhibition of assembly reactions, or induction of aberrant polymers.

Use of QSARs for activity prediction: unexpected relationship between the colchicine and paclitaxel sites

A major goal of this work was to determine whether structural features of known antimitotic agents would be useful in conjunction with computational methods in the identification of new cytotoxic agents with this mechanism of action. The QSARs developed from the learning set were, therefore, used to screen an unrelated data base containing the structures of 5000 chemicals. This search yielded 53 agents predicted to have significant interaction with tubulin. A significant number of these were obvious analogues of active agents in the learning set. To our initial surprise, paclitaxel (Fig. 7) was among the drugs selected in this search, which was based primarily on structural analysis of colchicine site agents. Several compounds judged to be sufficiently structurally distinct from known antimitotic agents were evaluated for effects on tubulin polymerization. Three of these had significant effects on the reaction. Two compounds[48] were weak inhibitors of assembly (IC_{50} values superstoichiometric to the tubulin concentration).

The third compound was discodermolide (Fig. 7), originally isolated from the marine sponge *Discodermia*

dissoluta. In studies described elsewhere, we found that (+)-discodermolide was more potent than paclitaxel, docetaxel, and 2-debenzoyl-2-*meta*-azidobenzoylpaclitaxel at promoting tubulin assembly and stabilizing tubulin polymers and caused mitotic arrest and spectacular microtubule bundle formation in cells in culture.[49]

Thus, although our initial computational search for new compounds was based on QSARs developed primarily from colchicine site agents, paclitaxel and the most active novel compound identified, discodermolide, enhance rather than inhibit tubulin polymerization. Figure 7 indicates the common MultiCASE biophore found in these two compounds shared with the colchicine site drugs (steganacin only). The CASE

biophore was imbedded in the MultiCASE biophore, and was found in two additional members of the learning set. We assume the failure to identify significant new colchicine site drugs is due, at least in part, to the limited scope of compounds in the 5000-member data base screened. We are presently screening larger structural data bases to identify more new tubulin interactive agents. More importantly, however, does the computational selection of paclitaxel and discodermolide indicate unsuspected overlap or coincidence of the binding site(s) for these polymer-stabilizing agents with the colchicine binding site?

Recent photoaffinity and tubulin-microtubule kinetic studies with colchicine and paclitaxel derivatives indicate this may indeed be the case. When the
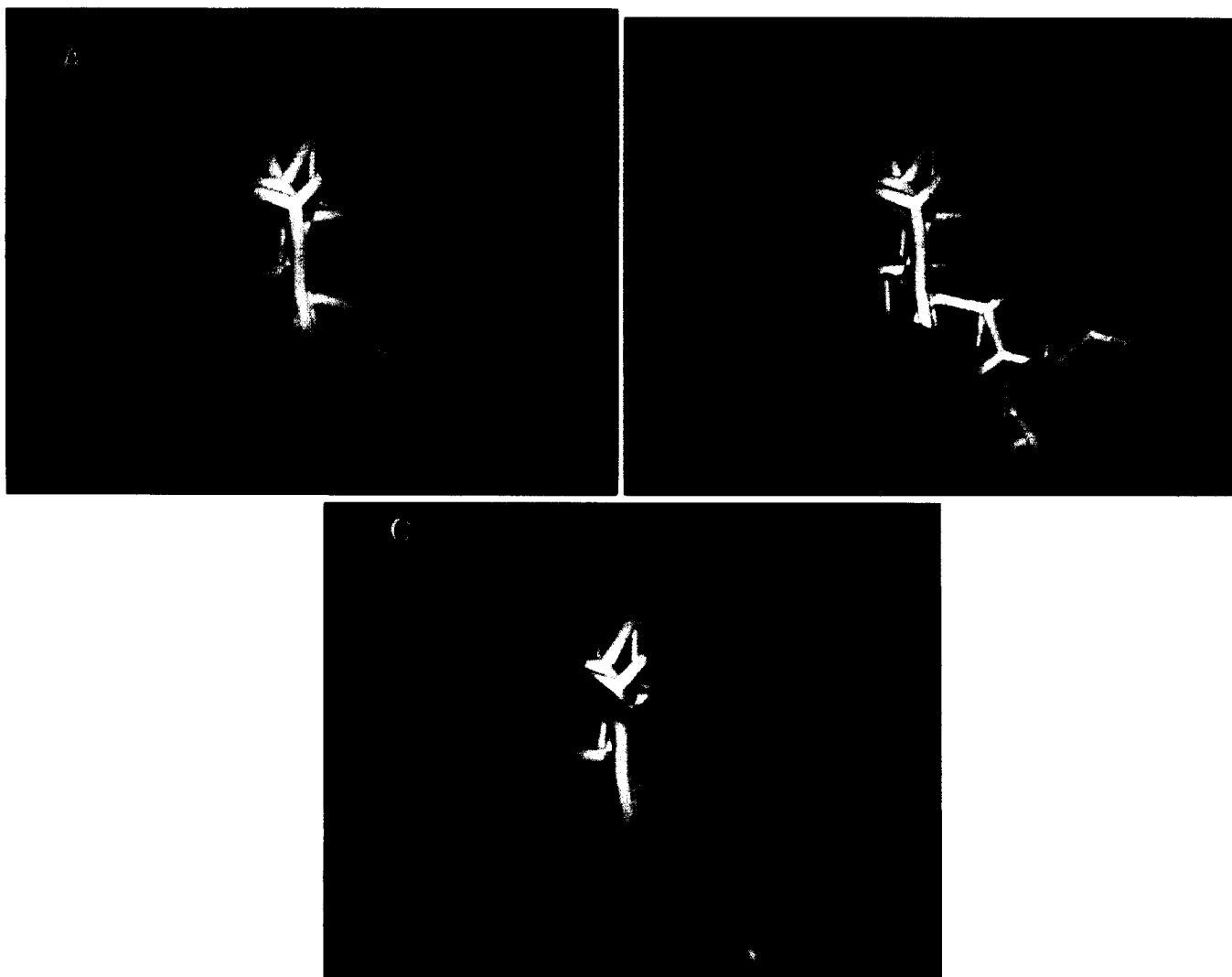

Figure 6. Hypothetical relative binding orientations of ligands at the colchicine binding site on tubulin. The models of colchicine (blue) and podophyllotoxin (white) were 'globally' minimized with CHARMm and AM1 as described in Materials and Methods and the isoelectronic atoms in the MultiCASE biophores shared by colchicinoids and podophylotoxins (see Discussion) were maximally superimposed to yield the overlaid structures in (A). (B) shows one of the energetically feasible potential binding orientations of combretastatin A-4 (yellow) with respect to colchicine and podophyllotoxin at the colchicine binding site. Combretastatin A-4 overlaps with the trimethoxyphenyl rings of both colchicine and podophyllotoxin in this orientation. (C) shows the hypothetical binding orientation of steganacin (red), with its biophore overlaid on the isoelectronic biophore atoms of colchicine and podophyllotoxin, at the colchicine binding site. The trimethoxyphenyl ring of steganacin overlaps with the trimethoxyphenyl ring of colchicine. The overall dimensions of the overlapping trinary system shown in (C) are 12.54 Å (podophyllotoxin trimethoxyphenyl to colchicine N-acetyl) × 11.81 Å (colchicine trimethoxyphenyl to steganacin acetate) × 13.03 Å (distance between colchicine and podophyllotoxin trimethoxyphenyl systems) × 11.51 Å (depth, roughly the length of the podophyllotoxin A-D ring system), the intersection volume is 35.5 Å^3, and the union volume 722.75 Å^3.
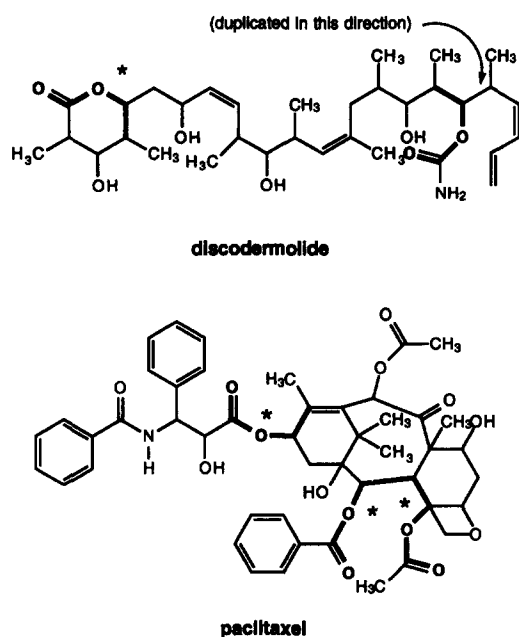
discodermolide

paclitaxel

Figure 7. Localization of the common MultiCASE biophore (bold) invoked to predict potent antitubulin activity for discodermolide and paclitaxel. The same biophore was found to be statistically significant in one colchicinoid, steganacin, and was located in its acetate side chain. Those marked with an asterisk (*) were accompanied by warnings due to being in an environment different from the biophore identified from the learning set.

tubulin–colchicine complex is illuminated at 350 nm (the absorbance maximum attributed to the colchicine tropolone moiety), covalent bonds form between the drug and two regions of β-tubulin (the peptide sequences 1–36 and 214–241).[50] Comparable results have been obtained with paclitaxel derivatives. A photoaffinity analogue of paclitaxel derivatized in the C_{13}-side chain reacts covalently with β-tubulin in the peptide sequence 1–31.[51] 2-Debenzoyl-2-*meta*-azido-benzoylpaclitaxel, originally synthesized as a photoactive derivative, reacts with β-tubulin in the peptide sequence 217–231.[52] Moreover, recent modeling studies predict that the C_2- and C_{13}-substituents of taxoids cluster hydrophobically when the drugs are in aqueous solution, with interhydrogen distances less than 5 Å.[53] Studies with the thermally-activated tubulin adducting agent 3-chloroacetyl-3-demethylthiocolchicine[54] show that the colchicine A-ring probably lies in the known 9 Å gap between Cys(239) and Cys(354) of β-tubulin,[55] suggesting that the tropolone C-ring lies between the region of the protein containing Cys(239) and the amino-terminus. These studies indicate that the binding site(s) for the tropolone moiety and the taxoid C_{13}/C_2 complex are in close proximity, if not identical. Additionally, colchicine, while depolymerizing microtubules as a thermodynamic requirement of the system, has been shown to kinetically stabilize microtubules in a paclitaxel-like manner.[56] When considered together, these data may explain the unanticipated success of our computational search, which was based largely on quantitative structure–activity relationships gleaned from colchicine site agents, in identifying a new and potent paclitaxel-mimetic compound.

Experimental

Tubulin polymerization inhibition assays were performed as previously described.[16,17,21]

QSAR analyses

The related CASE[18] and MultiCASE[19] (available from BIOSOFT International, South Euclid, OH) analyses were carried out on a DEC Alpha 3000/300x DECchip 21064 workstation. The structures of chemicals in the learning set and and their potencies in biological assays were obtained from several literature sources or were generated in this study.[2,8,10,14–17,20–34] For consistency and valid comparisons, literature data was taken from studies that included colchicine in evaluations. Thus, the reported in vitro tubulin polymerization inhibitory IC_{50} values for the chemicals, obtained in the cited studies generally with 10 μM bovine brain tubulin at 37 °C in the presence of microtubule associated proteins and GTP, were adjusted by relative ratios to reflect activities relative to a historic IC_{50} value for colchicine (2.4 μM). For some of the chalcones in the learning set,[20] an equivalent value calculated from the compound's antimitotic effect (37 °C, HeLa cells, 6 h) compared with that of 0.05 μg/mL colchicine was used.

Validation of QSARs

The validities of the resulting QSARs were determined by an exhaustive series of jackknife predictions on the chemicals in the learning set and subsequently applied to structures of known activity not in the learning set. The QSARs of the subgroups of chemicals discussed in detail in this manuscript were also reanalysed by the SAS System (SAS Institute Inc., Cary, North Carolina) and BMDP4R (BMDP Statistical Software, Inc., Los Angeles, California) suites of programs to provide verification of the reliability of the data and to cross-validate the regressions.

Molecular modeling

Molecular models were generated using the QUANTA molecular modeling package (Versions 3.3 or 4.0, Molecular Simulations, Inc., Burlington, Massachusetts) running on a Silicon Graphics IRIS Indigo Elan R3000 workstation by molecular mechanics minimization of coordinates from the Cambridge Structural Database or from 2-D structures drawn with the ChemNote program. Models were minimized with the CHARMm (Version 22.2) parameter set to energy gradient-, energy value- and step value-tolerances of 0.01, 0 and 0 kcal $Å^{-1}$, respectively, with an initial step size of 0.02 kcal $Å^{-1}$. A conformational search of torsions in all rotatable bonds in a given model to select a 'global' minimum energy structure was done by the grid scan method at steps of 30° per step, with 2000 steps of conjugant gradient minimization applied to each step. Geometry optimization and energetics calculations were conducted on the minimum energy structures at the semiempirical quantum chemical level by

using the AM1 Hamiltonian as implemented in AMPAC [Quantum Chemistry Program Exchange, program no. 506(2.1)]. A dielectric constant of 1 was used in all calculations. Superposition of the geometry-optimized compounds was carried out in QUANTA using the rigid body fit to common frame method after matching the isoelectronic biophore atoms in each molecular model.

Supplementary material

Structures of compounds comprising the learning set (59 pages) and statistical validations of colchicinoid and podophyllotoxin QSARs (35 pages) are available from the corresponding author.

Acknowledgments

References

1. Hamel, E. *Med. Res. Rev.* **1996**, *16*, 207.

2. Lin, C. M.; Singh, S. B.; Chu, P. S.; Dempcy, R. O.; Schmidt, J. M.; Pettit, G. R.; Hamel, E. *Mol. Pharmacol.* **1988**, *34*, 200.

3. Lin, C. M.; Ho, H. H.; Pettit, G. R.; Hamel. E. *Biochemistry* **1989**, *28*, 6984.

4. Andreu, J. M.; Timasheff, S. N. *Biochemistry* **1982**, *21*, 534.

5. Andreu, J. M.; Timasheff, S. N. *Biochemistry* **1982**, *21*, 6465.

6. David-Pfeuty, T.; Simon, C.; Pantaloni, D. *J. Biol. Chem.* **1979**, *21*, 2392.

7. Lin, C. M.; Hamel, E. *J. Biol. Chem.* **1981**, *256*, 9242.

8. Loike, J. D.; Brewer, C. F.; Sternlicht, H.; Gensler, W. J.; Horwitz, S. B. *Cancer Res.* **1978**, *38*, 2688.

9. Kelleher, J. K. *Mol. Pharmacol.* **1977**, *13*, 232.

10. Liu, S.-Y.; Hwang, B.-D.; Haruna, M.; Imakura, Y.; Lee, K.-H.; Cheng, Y.-C. *Mol. Pharmacol.* **1989**, *36*, 78.

11. Batra, J. K.; Kang, G. J.; Jurd, L.; Hamel, E. *Biochem. Pharmacol.* **1988**, *37*, 2595.

12. Rosner, M.; Capraro, H.-G.; Jacobsen, A. E.; Atwell, L.; Brossi, A. *J. Med. Chem.* **1981**, *24*, 257.

13. Brossi, A.; Sharma, P. N.; Atwell, L.; Jacobsen, A. E.; Iorio, M. A.; Molinari, M.; Chignell, C. F. *J. Med. Chem.* **1983**, *26*, 1365.

14. Staretz, M. E.; Hastie, S. B. *J. Med. Chem.* **1993**, *36*, 758.

15. Muzaffar, A.; Brossi, A.; Lin, C. M.; Hamel, E. *J. Med. Chem.* **1990**, *33*, 567.

16. Cushman, M.; Nagarathnam, D.; Gopal, D.; Chakraborti, A. K.; Lin, C. M.; Hamel, E. *J. Med. Chem.* **1991**, *34*, 2579.

17. Cushman, M.; Nagarathnam, D.; Gopal, D.; He, H.-M.; Lin, C. M.; Hamel, E. *J. Med. Chem.* **1992**, *35*, 2293.

18. Klopman, G. *J. Am. Chem. Soc.* **1984**, *106*, 7315.

19. Klopman, G. *Quant. Struct. Act. Relat.* **1992**, *11*, 176.

20. Edwards, M. L.; Stemerick, D. M.; Sunkara, P. S. *J. Med. Chem.* **1990**, *33*, 1948.

21. Sun, L.; McPhail, A. T.; Hamel, E.; Lin, C. M.; Hastie, S. B.; Chang, J.-J.; Lee, K.-H. *J. Med. Chem.* **1993**, *36*, 544.

22. Getahun, Z.; Jurd, L.; Chu, P. S.; Lin, C. M.; Hamel, E. *J. Med. Chem.* **1992**, *35*, 1058.

23. Batra, J. K.; Jurd, L.; Hamel, E. *Mol. Pharmacol.* **1985**, *27*, 94.

24. Saltarelli, D; Pantaloni, D. *Biochemistry* **1982**, *21*, 2996.

25. Hoebeke, J.; Nijen, G. V. *Life Sci.* **1975**, *17*, 591.

26. Barham S. S.; Brinkley B. R. *Cytobios* **1976**, *15*, 85.

27. Jiang, J. B.; Hesson, D. P.; Dusak, B. A.; Dexter, D. L.; Kang, G. J.; Hamel, E. *J. Med. Chem.* **1990**, *33*, 1721.

28. Cushman, M.; He, H. M.; Lin, C. M.; Hamel, E. *J. Med. Chem.* **1993**, *36*, 2817.

29. Kuo, S.-C.; Lee, H.-Z.; Juang, J.-P.; Lin, Y.-T.; Wu, T.-S.; Chang, J.-J.; Lednicer, D.; Paull, K. D.; Lin, C. M.; Hamel, E.; Lee, K.-H. *J. Med. Chem.* **1993**, *36*, 1146.

30. Solary, E.; Leteurtre, F.; Paull, K. D.; Scudiero, D.; Hamel, E.; Pommier, Y. *Biochem. Pharmacol.* **1993**, *45*, 2449.

31. D'Amato, R. J.; Lin, C. M.; Flynn, E.; Folkman, J.; Hamel, E. *Proc. Natl. Acad. Sci. U.S.A* . **1994**, *91*, 3964.

32. Li, L.; Wang, H.-K.; Kuo, S.-C.; Wu, T.-S.; Lednicer, D.; Lin, C. M.; Hamel, E.; Lee, K.-H. *J. Med. Chem.* **1994**, *37*, 1126.

33. Hamel, E.; ter Haar, E.; Jonnalagadda, S. S.; Magarian, R. A.; Griffin, M. T., Day, B. W., unpublished observations.

34. Hamel, E., unpublished observations.

35. Boye, O.; Itoh, Y.; Brossi, A.; Hamel, E. *Helv. Chim. Acta* **1989**, *72*, 1690.

36. Andreu, J. M.; Gorbunoff, M. J.; Lee, J. C.; Timasheff, S. N. *Biochemistry* **1984**, *23*, 1742.

37. Pyles, E. A.; Hastie, S. B. *Biochemistry* **1993**, *32*, 2329.

38. Boye, O.; Brossi, A.; Yeh, H. J. C.; Hamel, E.; Wegrzynski, B.; Toome, V. *Can. J. Chem.* **1992**, *70*, 1237.

39. Hastie, S. B. *Pharmac. Ther.* **1991**, *51*, 377.

40. Hamel, E.; Ho, H. H.; Kang, G.-J.; Lin, C. M. *Biochem. Pharmacol.* **1988**, *37*, 2445.

41. Batra, J. K.; Jurd, L.; Hamel, E. *Biochem. Pharmacol.* **1986**, *35*, 4013.

42. Brossi, A.; Yeh, H. J. C.; Chrzanowska, M.; Wolff, J.; Hamel, E.; Lin, C. M.; Quinn, F.; Suffness, M.; Silverton, J. *Med. Res. Rev.* **1988**, *8*, 77.

43. We have found 4'-demethylpodophyllotoxin (obtained from Bristol-Myers) to be about fourfold less active than podophyllotoxin as an inhibitor of tubulin assembly (Hamel, E., unpublished observations).

44. Terada, T.; Fujimoto, K.; Nomura, M.; Yamashita, J.; Kobunai, T.; Takeda, S.; Wierzba, K.; Yamada, Y.; Yamaguchi, H. *Chem. Pharm. Bull.* **1992**, *40*, 2720.

45. E. Hamel, unpublished observations. See also ref 4. It should also be noted that the most active benzylbenzodioxole derivatives inhibit tubulin-dependent GTP hydrolysis,[37,46] while the methylenedioxybenzopyran derivatives stimulate GTP hydrolysis.[13]

46. Sackett, D. L. *Pharmac. Ther.* **1993**, *59*, 163.

47. Zavala, F.; Guenard, D.; Robin, J.-P.; Brown, E. *J. Med. Chem.* **1980**, *23*, 546.

48. These were 3-nitrocarbazole (provided by Professor Louise Ball, University of North Carolina) and eupatoriopi-crin (provided by Dr. Herman Woerdenbag, State University of Groningen).

49. ter Haar, E.; Kowalski, R. J.; Hamel, E.; Lin, C. M.; Longley, R. E.; Gunasekera, S. P.; Rosenkranz, H. S.; Day, B. W. *Biochemistry* **1996**, *35*, 243.

50. Uppuluri, S.; Knipling, L.; Sackett, D. L.; Wolff, J. *Proc. Natl. Acad. Sci. U.S.A.* **1993**, *90*, 11598.

51. Rao, S.; Krauss, N. E.; Heerding, J. M.; Swindell, C. S.; Ringel, I.; Orr, G. A.; Horwitz, S. B. *J. Biol. Chem.* **1994**, *269*, 3132.

52. Rao, S.; Orr, G. A.; Chaudhary, A. G.; Kingston, D. G. I.; Horwitz, S. B. *J. Biol. Chem.* **1995**, *270*, 20235.

53. Vander Velde, D. G.; Georg, G. I.; Grunewald, G. L.; Gunn, C. W.; Mitscher, L. A. *J. Am. Chem. Soc.* **1993**, *115*, 11650.

54. Bai, R.; Pei, X.-F.; Boye, O.; Getahun, Z.; Grover, S.; Nguyen, N. Y.; Brossi, A.; Hamel, E. *J. Biol. Chem.* **1996**, *271*, 12639.

55. Ludueña, R. F.; Roach, M. C. *Pharmac. Ther.* **1991**, *49*, 133.

56. Panda, D.; Daijo, J. E.; Jordan, M. A.; Wilson, L. *Biochemistry* **1995**, *34*, 9921.